

Jennifer W. MacAdam · John H. Grabber

## Relationship of growth cessation with the formation of diferulate cross-links and *p*-coumaroylated lignins in tall fescue leaf blades

Received: 14 January 2002 / Accepted: 26 April 2002 / Published online: 14 June 2002  
© Springer-Verlag 2002

**Abstract** We examined relationships among cell wall feruloylation, diferulate cross-linking, *p*-coumarate deposition, and apoplastic peroxidase (EC 1.11.1.7) activity with changes in the elongation rate of leaf blades of slow and rapid elongating genotypes of tall fescue (*Festuca arundinacea* Schreb.). Growth was not directly influenced by ferulic acid deposition but leaf elongation decelerated as 8–5-, 8–O–4-, 8–8-, and 5–5-coupled diferulic acids accumulated in cell walls. Growth rapidly slowed and stopped with the deposition of *p*-coumarate, which is primarily associated with lignification in grass cell walls. Accretion of ferulate, diferulates and *p*-coumarate continued after growth ended, into the later stages of secondary wall formation. The concentration of 8-coupled diferulates dwarfed that of the more commonly measured 5–5-coupled isomer, suggesting that the latter dimer is a poor indicator of diferulate cross-linking in cell walls. Further work is required to clearly demonstrate the role of diferulate cross-linking and *p*-coumaroylated lignins in the cessation of leaf growth in grasses.

**Keywords** Cell elongation · Cell wall cross-linking · Diferulate · Ferulate · *Festuca* (cell wall) · Lignin

**Abbreviations** LER: leaf elongation rate · SER: segmental elongation rate

### Introduction

Markwalder and Neukom (1976) demonstrated that 5–5-coupled diferulic acid was formed by peroxidase/H<sub>2</sub>O<sub>2</sub>-mediated oxidation of ferulic acid esters on arabinoxylans. In the same study, they demonstrated the natural occurrence of 5–5-coupled diferulic acid in wheat endosperm. Ishii (1991) confirmed the existence of the 5–5-coupled diferuloyl arabinoxylan hexasaccharide in bamboo [*Phyllostachys edulis* (Carrière) J. Houz.]. The discovery of diferulic acid linkages between adjacent feruloylated xylan chains led to the hypothesis that such bonds control cell wall extensibility (Fry 1979) and numerous studies have demonstrated a correlation between an increase in the content of 5–5-coupled diferulic acid in cell walls of gramineous coleoptiles and a decrease in growth and cell wall extensibility (e.g. Kamisaka et al. 1990; Tan et al. 1991, 1992; Wakabayashi et al. 1997; Gonzalez and Rojas 1999; Gonzalez et al. 1999; Kawamura et al. 2000). In these studies, the ratio of 5–5-coupled diferulic acid to ferulic acid remained fairly constant, even as growth rate or extensibility changed dramatically.

Ralph et al. (1994b) demonstrated that the 5–5-coupled dimer represents only a small portion of the dehydrodiferulates formed in grass walls; concentrations of 8–O–4-, 8–8-, and particularly 8–5-coupled diferulates usually exceed that of 5–5-coupled diferulate. Recent studies also indicate that 5–5-coupled diferulate, unlike 8-coupled dimers, is probably formed by intramolecular dimerization of ferulate polysaccharide esters (Hatfield and Ralph 1999). Therefore, most if not all cross-linking mediated by ferulic acid involves 8–O–4-, 8–8-, and 8–5-coupled diferulates, yet relationships between 8-coupled diferulates and cell wall extension have been ignored, even in recent studies with cereal coleoptiles.

Lignification of primary walls has also been associated with reduced extensibility and growth of coleoptiles (Musel et al. 1997; Schopfer et al. 2001). Lignins in grasses are acylated with *p*-coumarate, which is attached

J.W. MacAdam (✉)  
Department of Plants, Soils, and Biometeorology,  
Utah State University, Logan, UT 84322-4820, USA  
E-mail: jenmac@cc.usu.edu  
Fax: +1-435-797-3376

J.H. Grabber  
U.S. Dairy Forage Research Center,  
Agricultural Research Service – U.S. Department of Agriculture,  
1925 Linden Drive West, Madison, WI 53706, USA

primarily to syringyl units (Ralph et al. 1994a; Grabber et al. 1996; Lu and Ralph 1999). Although very small quantities of *p*-coumarate are esterified to arabinoxylans in immature tissues, most *p*-coumarate accretion occurs in tandem with lignification (Musel et al. 1997; Morrison et al. 1998; Vailhé et al. 2000), making *p*-coumarate accumulation a convenient indicator of lignification. During lignification, cell walls are further stiffened by oxidative coupling of ferulate monomers and dimers with monolignols, forming additional cross-links between structural polysaccharides and lignin (Grabber et al. 1995, 2000). In contrast, *p*-coumarate is averse to participating in oxidative coupling, forming few if any cross-linked structures in lignified cell walls (Ralph et al. 1994a; Vailhé et al. 2000). Therefore, any association between growth and *p*-coumarate deposition is probably related to cell wall lignification.

In previous work, we observed that the elongation rate of epidermal cells of tall fescue leaf blades increases exponentially and then stops abruptly (MacAdam et al. 1989), implying a rapid change in cell-wall mechanical properties. Therefore, the primary objective of our current study was to investigate relationships between the cell wall deposition of ferulate monomers, all major diferulates, and *p*-coumarate with changes in the segmental elongation rate (SER) of tall fescue leaf blades. Two genotypes with differing growth characteristics were used in the study to determine whether growth cessation of leaves was consistently associated with the deposition of *p*-hydroxycinnamates.

Since peroxidase activity is required for the formation of diferulates and lignin (Grabber et al. 1995, 2000), we also compared the appearance of an apoplastic peroxidase, as reported in a previous study of the same tall fescue genotype (MacAdam et al. 1992), with the accretion of diferulates and lignin in cell walls of leaf blades. Previous work with tall fescue and maize (*Zea mays* L.) leaves demonstrated a transient increase in apoplastic peroxidase that occurs as epidermal cell elongation slows and stops (MacAdam et al. 1992; de Souza and MacAdam 1998, 2001).

## Materials and methods

### Plant culture

Vegetatively propagated tillers were used to produce numerous clones of two genotypes of tall fescue (*Festuca arundinacea* Schreb.) selected for high and low leaf elongation rates (LERs; Jones et al. 1979). The high-LER genotype consistently exhibits a 50% greater LER than that of the low-LER genotype under a variety of environmental conditions. Plants were grown in 12-cm-deep by 15-cm-diameter pots in Terra-Lite Redi-Earth Peat-Lite potting mix (Scotts-Sierra Horticultural Products Co., Marysville, Ohio, USA) in a controlled-environment chamber at 22/17 °C day/night temperature, 15-h daylength, and 400  $\mu\text{mol photons m}^{-2} \text{s}^{-1}$  photosynthetically active radiation (PAR). Pots of tillers were replicates, and three pots of the high-LER and two pots of the low-LER genotypes were randomly arranged in one growth chamber for the duration of the experiment, and fertilized at 6-week intervals with a solution containing 1  $\text{g l}^{-1}$  N, 0.46  $\text{g l}^{-1}$  P, 0.87  $\text{g l}^{-1}$  K, and 0.15  $\text{g l}^{-1}$  S.

At the time of destructive sampling, each pot contained 54–92 elongating leaf blades at approximately the same stage of development.

### Estimation of cell elongation rates

Prior to destructive sampling, mean daily elongation rates of leaves of both genotypes were calculated by measuring the length of nine leaves over a 5-day period following leaf emergence. During this time, leaf growth rate is constant (Vassey 1986). At the time of destructive sampling, polyvinylformaldehyde (Formvar; Ted Pella Inc., Redding, Calif., USA) replicas of intercostal abaxial epidermal cells were made of four leaves from each pot. To form replicas, a thin film of 4% (w/v) Formvar in chloroform was applied to the leaf using a camelhair brush and allowed to dry briefly. A strip of clear cellophane adhesive tape was applied to the leaf, the replica was lifted off, and the cellophane tape and replica were applied to a glass microscope slide (Schnyder et al. 1990). Formvar has been routinely used to make replicas for electron microscopy, and accurately reproduces surface features without distortion (Schaefer and Harker 1942). Epidermal cell length data were derived from at least two Formvar replicas per pot. The length of at least five intercostal epidermal cells was measured at each location on each replica starting 2.5 mm distal to the ligule. Segmental elongation rates were calculated from LERs and cell length profiles using a relationship derived from the continuity equation. Epidermal cell division occurs only within the basal 2 mm of the leaf blade (MacAdam et al. 1989). In regions of the leaf where no cell division occurs, the relationship between cell length and the velocity of displacement of tissue from the ligule can be expressed as  $V_A = (V_F/L_F) L_A$ , where  $V_A$  is displacement velocity ( $\mu\text{m h}^{-1}$ ) and  $L_A$  is cell length ( $\mu\text{m}$ ) at a point A distal to the ligule.  $V_F$  and  $L_F$  are final velocity (or leaf elongation rate) and final cell length, respectively (Scott et al. 1968; Carmona and Cuadrado 1986; Silk et al. 1989). A third-order polynomial equation was fitted to values of  $V_A$  and plotted against location distal to the ligule. Segmental elongation rates ( $\text{mm mm}^{-1} \text{h}^{-1}$ ) were calculated from the first derivative of the equation fitted to  $V_A$  (Silk et al. 1989). To plot data on a temporal basis, the time required for a cell to be displaced through successive 2.5-mm intervals was calculated by dividing the distance interval by the mean displacement velocity for that interval, and successive time intervals were summed. The time at which SER reached a maximum was estimated by solving a quadratic equation fit through SER points adjacent to the maximum. Similar methods were used to estimate the time at which cell wall mass reached a minimum. The time at which SER transitioned from an increasing rate of increase to a declining rate of increase was estimated by solving a quadratic equation fit through the first derivative of SER points. The first derivative of each point of the SER curve was calculated by fitting a quadratic equation through that point and its nearest neighbors.

### Preparation of cell walls and analysis of *p*-hydroxycinnamates

At sampling, elongating leaf blades had a length approximately half that of mature leaf blades. At this stage of development, the ligule had differentiated at the base of leaves, about 1 mm from the point of attachment of the leaf to the stem; but no sheath elongation had occurred. Leaves were detached and cut into 5-mm segments from the ligule toward the leaf tip. The basal 60 mm of the low-LER genotype and the basal 90 mm of the high-LER genotype were sampled for this study. Freshly harvested leaf blade segments from each replication were frozen in liquid nitrogen, ground using a mortar and pestle, and extracted successively with ice-cold 50 mM phosphate buffer pH 7 (four times), acetone (four times), 2:1 (v/v) chloroform:methanol (twice), and finally acetone (twice) to prepare cell walls. Cell walls isolated from all segments from the high-LER genotype and the basal 45 mm of the low-LER genotype were analyzed for alkali-labile *p*-hydroxycinnamates.

Briefly, all cell walls collected from each segment (10–45 mg) were incubated at room temperature in 1.5 ml of 2 M aqueous NaOH under N<sub>2</sub> for 20 h. 2-Hydroxycinnamate (0.1 mg) was added as an internal standard. After acidification (pH < 2), samples were extracted three times with one volume of ether. Extracts were combined, dried, silylated and then analyzed by GC-FID (Ralph et al. 1994b). A segmented quadratic-plateau regression model was used to estimate the time at which the deposition of *p*-hydroxycinnamates began and ended during leaf development (SAS Institute Inc., Cary, N.C., USA). This model was also used to estimate the time at which cell wall deposition ended during leaf development. The segmented model gave an excellent fit to the data, explaining at least 98% of the variation in *p*-hydroxycinnamate and cell wall accretion.

## Results and discussion

### Dynamics of leaf blade elongation and cell wall deposition

In elongating grass leaf blades, longitudinal files of cells undergo division at the base of the leaf blade and are displaced toward the leaf tip by ongoing cell division and elongation. Distal to the elongation zone, continuing basal elongation causes displacement of tissues through the zone of secondary cell wall deposition (MacAdam et al. 1989). Growth of tissues that comprise the leaf (mesophyll, vascular, structural, and epidermal) is coordinated because interior leaf cells remain radially connected from the vascular tissue to the epidermis via plasmodesmata established during cell division. Division of mesophyll cells continues after division of epidermal cells has stopped (MacAdam et al. 1989), and this continued division and the development of air spaces among mesophyll cells allows radial cell-to-cell connections to be maintained as leaves elongate despite differences in final cell size. With the exception of intrusive tip growth of fibers, cells at a given distance from the ligule cease elongation together and, therefore, we monitored change in epidermal cell length to assess overall leaf growth. The location of the zones of elongation and secondary cell wall deposition, in relation to the time at which epidermal cell elongation ends, is illustrated for the high-LER genotype in Fig. 1. The rate of displacement of a given epidermal cell increases with position

along the leaf blade from the meristem at the base through the distal end of the elongation zone because a constant elongation rate is acting on cells of increasing length (Erickson 1976). In tissue that is displaced into the zone of secondary cell wall deposition, cells are no longer elongating and the rate of displacement due to continuing cell division and elongation at the leaf base becomes constant (Fig. 1).

Overall, leaf elongation rate averaged 1.35 mm h<sup>-1</sup> for the high-LER genotype and 0.54 mm h<sup>-1</sup> for the low-LER genotype. The length of the elongation zone, determined from cell length profiles, was about 22 mm for both genotypes (Fig. 2). This is in contrast to earlier

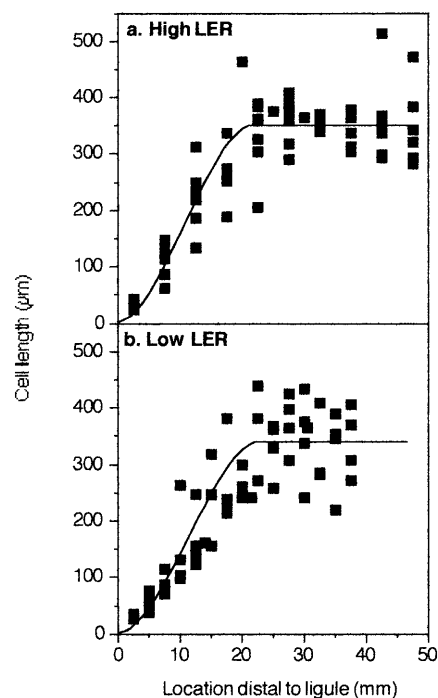
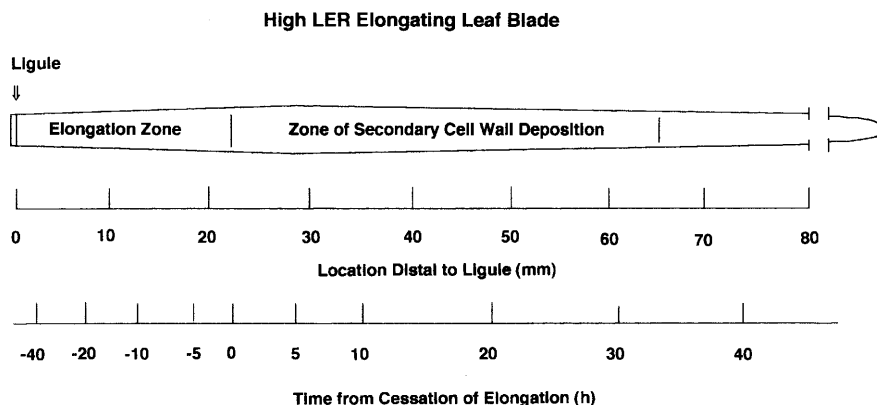


Fig. 2. Epidermal cell length data from two Formvar replicas per pot of elongating leaf blades from the high-LER (a) and low-LER (b) genotypes of tall fescue. Each pot was a replication for assay of *p*-hydroxycinnamic acids, but cell length data are pooled in this figure. Each datum is the mean of at least five intercostal abaxial epidermal cells

Fig. 1. Diagram of an elongating tall fescue (*Festuca arundinacea*) leaf blade illustrating the gradient of development from the leaf base to the leaf tip, with distances and times indicated for the high-LER genotype of tall fescue



studies in which the length of the elongation zone of the high-LER genotype was about 50% greater than that of the low-LER genotype (e.g. MacAdam et al. 1989), the elongation-zone length of the low-LER genotype in this study did not differ from that of the high-LER genotype. The change reported from earlier studies was due to a shading effect from high plant population density in the current study in low-LER plants, which tiller more prolifically and were 2 weeks older than high-LER plants. Final cell lengths were also similar for both genotypes, averaging 350  $\mu\text{m}$  (Fig. 2). Residence times of epidermal cells in the meristem and elongation zones averaged 140 h for the high-LER genotype and 400 h for the low-LER genotype. A segmental elongation rate (SER) for each genotype was derived from pooled cell length data (Fig. 2). The SER of both genotypes initially increased at an increasing rate and then transitioned to a declining rate of increase at about -21 h (time to cessation of elongation) in the high-LER genotype and at about -52 h in the low-LER genotype (Fig. 3). SER reached a maximum of 0.089  $\text{mm mm}^{-1} \text{h}^{-1}$  at about -11 h in the high-LER genotype and 0.036  $\text{mm mm}^{-1} \text{h}^{-1}$  at about -28 h in the low-LER genotype. After reaching a maximum, SER declined rapidly as leaf tissue stopped elongating.

Deposition of cell walls and *p*-hydroxycinnamic acids into leaf blades

Cell wall dry mass per millimeter leaf length initially decreased toward the distal end of the elongation zone as end wall density per millimeter decreased with cell elongation (Fig. 3), reaching a minimum within a few hours of cessation of elongation in both genotypes. Cell wall mass then increased, due to secondary cell wall deposition (MacAdam and Nelson 1987), ending about 46 h after elongation ceased in the high-LER genotype. In the low-LER genotype, secondary cell wall deposition continued beyond the last sampling time at 64 h; regression analysis indicated that cell wall deposition ended about 97 h after cell elongation ended. The higher cell wall mass per millimeter of the high-LER genotype is due to the greater leaf width and thickness of this genotype.

Accretion of ferulate and diferulates in cell walls of high-LER leaf blades began about 23 h before elongation stopped (Fig. 4a). In the low-LER genotype, ferulate accretion began about 67 h before elongation ceased (Fig. 4b). The accumulation of diferulic acids in the low-LER genotype was delayed, beginning about 14 h later; the expanded time frame of low-LER elongation allowed a better resolution of these two cell wall components. In both genotypes, deposition of diferulates into cell walls began within 1 or 2 h of the time when SER transitioned from an increasing to a declining rate of increase. Peroxidase-mediated dimerization of ferulate into diferulates probably occurs mainly in cell walls, although some dimerization can occur within Golgi vesicles just prior to xylan deposition into the apoplastic space (Myton and Fry 1995; Fry et al. 2000). Diferulate cross-linking is commonly thought to play a role in rigidifying walls and decelerating growth.

Due to limited quantities, cell walls were used only for the analysis of *p*-hydroxycinnamates; lignins were not determined by typical gravimetric or spectrophotometric procedures. One *p*-hydroxycinnamate, *p*-coumarate, is however a major component of grass lignin and its accumulation in tissue may be used as an indicator of lignin deposition (Musel et al. 1997; Morrison et al. 1998; Vailhé et al. 2000). During our analyses, we observed (data not shown) that *p*-coumarate accretion corresponded with the appearance of dimeric cross-products between ferulate and the lignin precursor coniferyl alcohol (Jacquet et al. 1995), providing further evidence that *p*-coumarate accretion is linked to lignification. The deposition of *p*-coumarate began later in leaf development than diferulates, about 10 and 32 h before elongation ceased in the high- and low-LER genotypes, respectively (Fig. 4). Accretion of *p*-coumarate, and therefore of *p*-coumaroylated lignins, began at about the time SER reached a maximum and then rapidly declined to zero.

These results, using genotypes with differing growth characteristics, suggest leaf elongation is slowed somewhat at the onset of diferulate cross-linking and ended

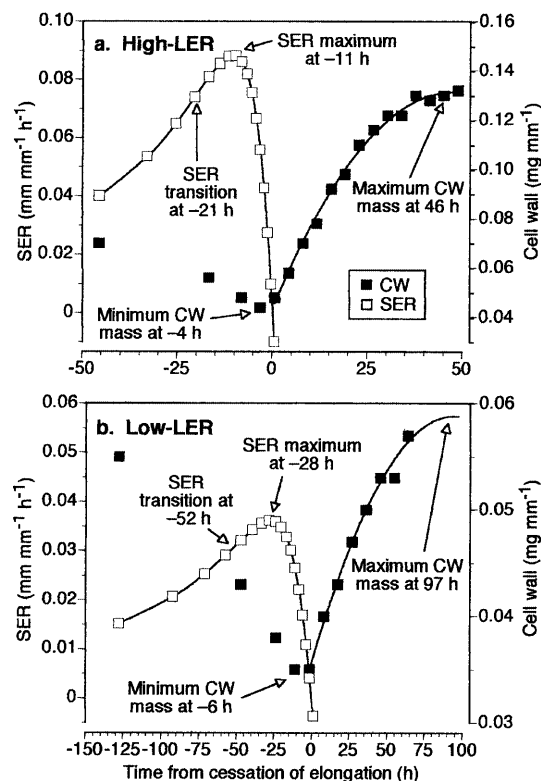


**Fig. 3.** Segmental elongation rates (SER) and mass of cell walls (CW) of leaf blades from the high-LER (a) and low-LER (b) genotypes of tall fescue. Data are plotted at the centers of 5-mm-long leaf blade segments. The segmented curves used to predict the time of maximum CW accretion are indicated on the figure

by the deposition of *p*-coumaroylated lignin in cell walls. The role of ferulates in ending growth may, however, be greater than indicated by this analysis since incorporation of ferulate and diferulate xylan esters into lignin dramatically increases ferulate-mediated cross-linking of cell walls (Grabber et al. 2000). Indeed this type of cross-linking may represent a primary mechanism by which lignin reduces cell wall extensibility. The temporal association of ferulate cross-linking with cessation of leaf elongation does not, however, demonstrate a cause-and-

effect relationship. Kamisaka et al. (1990), among others, suggest that polysaccharide feruloylation and diferulate cross-linking limit cell expansion by restricting cell-wall enzymatic hydrolysis. Diferulate cross-linking would also limit expansion by rigidifying the cell wall. Although several studies indicate that diferulates serve these roles (Schopfer 1996; Grabber et al. 1998a, b), there is little or no evidence that feruloylation markedly alters the mechanical properties of structural polysaccharides or their susceptibility to enzymatic hydrolysis.

The cell wall concentration of ferulate and diferulates in the high-*LER* genotype reached a maximum about 12 h after elongation ended (Fig. 4a). Diferulate concentration then remained constant while ferulate concentration declined 17% as cell wall mass increased by an additional 63% (Fig. 3a). In other studies, cell wall concentrations of ferulate were also reported to decline during secondary wall formation in grass internodes. This reduction in measurable ferulate during secondary wall formation has been used to support the contention that most, if not all, ferulates are deposited in primary cell walls (Terashima et al. 1993; Jung et al. 1998). However, secondary cell wall deposition continues until approximately 46 h in the high-*LER* genotype (Fig. 3a), and when data for this genotype are plotted on a  $\text{mg mm}^{-1}$  basis (Fig. 5), it is clear that the deposition of ferulate and particularly diferulates continues into the later stages of secondary cell wall formation, 34 and 46 h, respectively. Indeed data for the high-*LER* genotype indicate that at least 70% of alkali-labile total ferulates (monomers and dimers) were deposited during secondary wall formation. Immunocytochemical studies with maize stems also indicate that ferulates are deposited mainly in lignified walls of secondarily thickened xylem, sclerenchyma, phloem fibers, and parenchyma tissues (Migne et al. 1998).

Our analyses, however, probably underestimate the concentrations of ferulate and diferulates deposited during secondary wall deposition. As mentioned earlier, ferulate and diferulates readily co-polymerize with

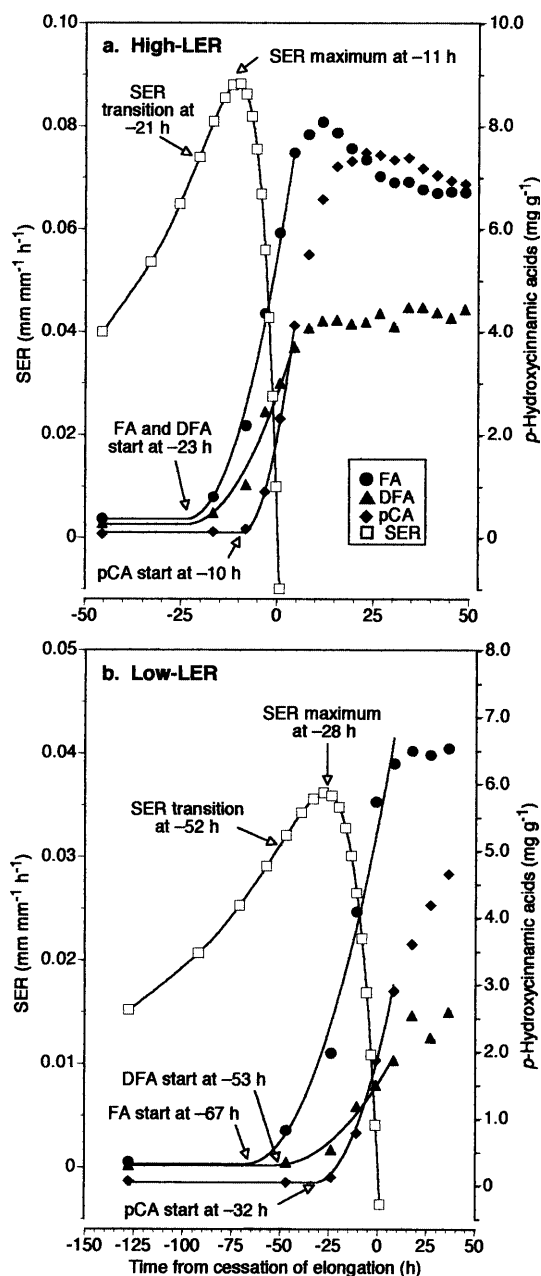


**Fig. 4.** Segmental elongation rate (*SER*) and cell wall concentrations of ferulate (*FA*), diferulates (*DFA*), and *p*-coumarate (*pCA*) in leaf blades from the high-*LER* (a) and low-*LER* (b) genotypes of tall fescue. The segmented curves used to predict the start times of *p*-hydroxycinnamate accretion are indicated on the figure

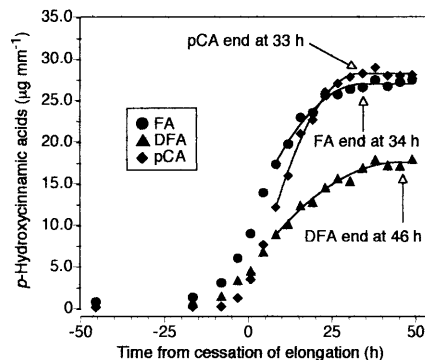


**Fig. 5.** Per-unit-length contents of ferulate (*FA*), diferulates (*DFA*), and *p*-coumarate (*pCA*) in leaf blades from the high-*LER* genotype of tall fescue. The segmented curves used to predict the end times of *p*-hydroxycinnamate accretion are indicated on the figure

monolignols, cross-linking feruloylated xylans to lignin. Once incorporated into lignin, ferulate and diferulates are not released from cell walls by room-temperature alkaline hydrolysis. Indeed, most ferulate- and diferulate-lignin cross-links are not cleaved even by high-temperature alkaline hydrolysis or by other solvolytic methods currently used to estimate such cross-linking in cell walls (Grabber et al. 2000). Ferulate and the various diferulate isomers also incorporate into lignin at differing rates, altering the apparent abundance and ratio of these *p*-hydroxycinnamates in cell walls. Therefore, researchers should exercise caution when relating ferulate or diferulate concentrations to cell wall extensibility or growth if lignification of coleoptiles or other tissues has commenced.

*p*-Coumarate concentrations in cell walls of the high-LER genotype (Fig. 4a) also peaked midway through secondary cell wall formation, about 26 h after elongation ceased, and then declined about 7% until secondary cell wall deposition ended. When plotted on a  $\text{mg mm}^{-1}$  basis (Fig. 5), content of *p*-coumarate appears to plateau about 33 h after elongation ceased. In other studies with grass internodes (Scobbie et al. 1993; Vailhé et al. 2000), a modest decline in cell wall *p*-coumarate is also evident at the later stages of secondary wall formation and lignification. Since *p*-coumarate is primarily a component of lignin, these observations may indicate that lignification stops before secondary wall formation is complete. An alternative interpretation is that acylation of monolignols by *p*-coumarate slows or stops at the later stages of lignification. Although the dataset for the low-LER genotype is less complete, similar patterns of ferulate, diferulate, and *p*-coumarate deposition during secondary wall formation are apparent (data not shown). In contrast to ferulate, *p*-coumarate esters on lignin units form few, if any, cross-linked structures mediated by radical coupling reactions (Ralph et al. 1994b). *p*-Coumarate (and ferulate) can, however, undergo a photocatalyzed cyclodimerization during tissue development to form truxillic and truxinic acids (Hartley et al. 1990; Hanley et al. 1993) but neither was detected in our cell wall preparations. Therefore, room-temperature alkaline hydrolysis, as used in this study, provides a good estimate of the total quantity of *p*-coumarate in walls and thereby the progress of lignification.

As observed in previous studies with grass cell walls (Ralph et al. 1994b; Grabber et al. 1995, 2000), the concentration of 8-coupled diferulates dwarfed that of the 5–5-coupled isomer in both genotypes (Fig. 6). During growth of the high-LER genotype, the concentrations of 8–5- and 8–*O*–4-coupled isomers increased 10-fold from –20 to +20 h from cessation of elongation, while concentrations of 8–8- and 5–5-coupled isomers increased only 5-fold over the same 40 h period. Similar differences in diferulate isomers were apparent from –50 to +50 h for the low-LER genotype. The proportion of diferulates in walls is controlled, in part, by the unpaired electron distribution of ferulate radicals, the relative energies of the coupling products, matrix effects, and the differing propensity of diferulates to co-polymerize into

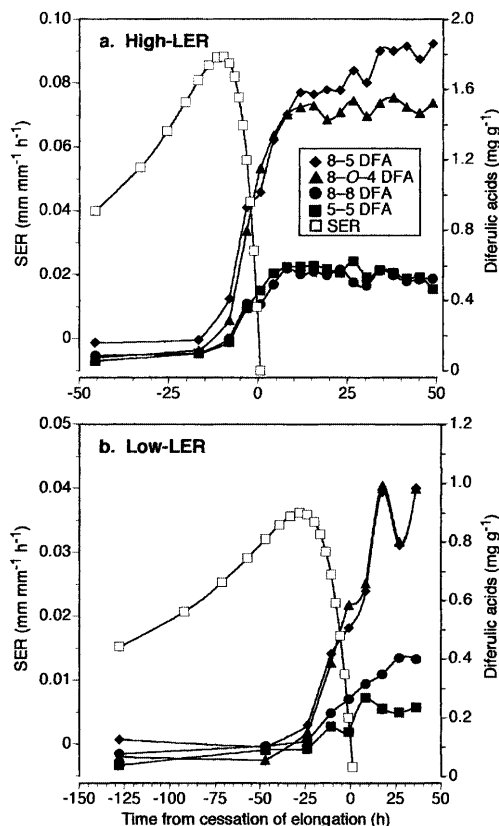
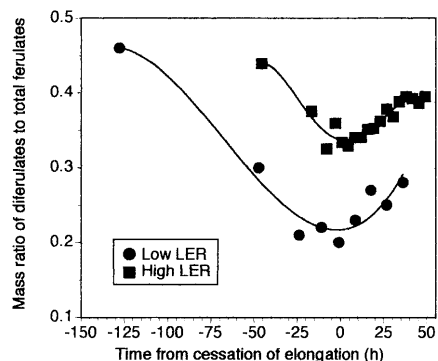


Fig. 6. Segmental elongation rates (SER) and cell wall concentrations of diferulate (DFA) isomers in leaf blades of the high-LER (a) and low-LER (b) genotypes of tall fescue

lignin (Elder and Ede 1995; Russell et al. 1996; Hatfield and Ralph 1999; Grabber et al. 2000). The 5–5-coupled isomer is frequently the only diferulate measured in growth studies, but since this dimer comprised only a small and variable proportion (12–17%) of the total diferulates in cell walls, we believe it is a poor indicator of diferulate cross-linking.

In studies with monocot coleoptiles (e.g. Kamisaka et al. 1990; Tan et al. 1991, 1992; Wakabayashi et al. 1997; Gonzalez et al. 1999; Kawamura et al. 2000), growth dynamics were related to cell wall feruloylation, as indicated by alkali-labile ferulate, or to changes in the ratio of ferulate to diferulate (apparently just the 5–5-coupled isomer). This approach is flawed for two reasons. First, estimation of wall feruloylation by ferulate levels ignores the fact that ferulates are depleted during the formation of dimers by photo- and oxidative-mediated processes (Hanley et al. 1993; Grabber et al. 1995, 2000). Feruloylation of nonlignified tissues is, therefore, best represented by the total concentration of ferulate monomers and dimers in cell walls. Second, as noted earlier, the 5–5-coupled isomer represents a small and variable proportion of the ferulate dimers formed in cell walls, greatly limiting its usefulness as an indicator of cross-linking. Therefore, analysis of all diferulate isomers must be undertaken to accurately reflect overall ferulate cross-linking in cell walls.



**Fig. 7.** Ratio of diferulates to total ferulates (monomers plus dimers) in leaf blades from the high-LER and low-LER genotypes of tall fescue

In our study, the ratio of diferulates to total ferulates (ferulate monomers plus dimers) declined from about 0.45 in the leaf meristem of both genotypes to 0.35 for the high-LER genotype and to 0.20 for the low-LER genotype when leaf elongation ended (Fig. 7). The proportion of diferulates to total ferulates then increased to an intermediate level during secondary wall formation. The decline in this ratio was due to a more rapid rate of ferulate deposition than ferulate dimerization as cells were displaced through the elongation zone. During secondary wall formation, the ratio of diferulates to total ferulates increased, perhaps because of preferential incorporation of ferulate monomers over diferulates into lignin (Grabber et al. 2000). These observations, combined with the lack of synchrony between ferulate accretion and changes in SER, indicate that changes in the ratios of ferulates and diferulates or wall feruloylation do not directly control growth as has been suggested in some studies with coleoptiles (Tan et al. 1991; Wakabayashi et al. 1997).

A transient increase in apoplastic peroxidase precedes cessation of segmental elongation in both tall fescue (MacAdam et al. 1992) and maize (de Souza and MacAdam 1998, 2001). In a previous study using the same low- and high-LER genotypes of tall fescue under similar controlled-environment chamber conditions of daylength, light and temperature (MacAdam et al. 1992), the SER of the low-LER genotype changed over time almost identically to the same clonal material in this study (Fig. 8a). Therefore, we have compared changes in apoplastic peroxidase activity from the previous study with the deposition of *p*-hydroxycinnamates into cell walls in the current study (Fig. 8b). In the earlier study the accumulation of apoplastic peroxidase began at about -60 h and peaked at about -20 h from cessation of elongation. The accumulation of ferulate in cell walls in the present study began at about -67 h and the onset of ferulate dimerization at about -53 h, while *p*-coumarate began to accumulate at -32 h. Therefore, the formation of diferulates appears to begin at about the time apoplastic peroxidase activity appears in the cell wall. Gonzales et al. (1999) also noted the appearance of

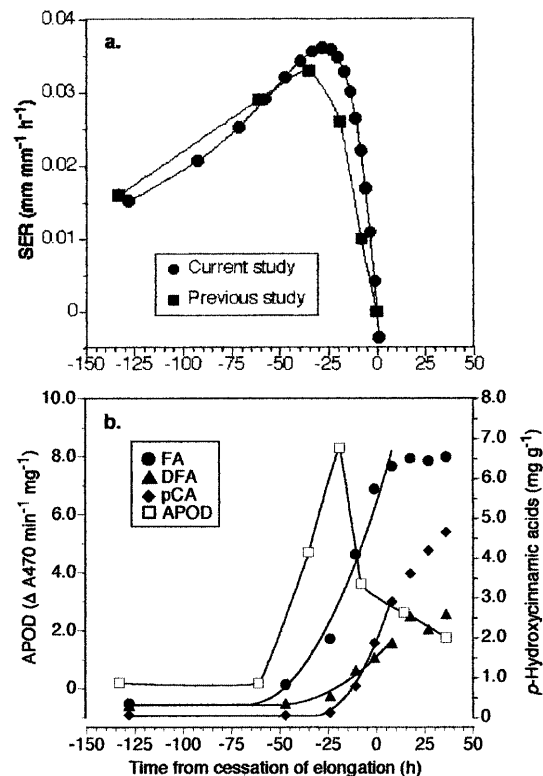


**Fig. 8.** **a** Segmental elongation rates (*SER*) of genetically identical low-LER leaf blades of tall fescue from the current study and from a previous study (MacAdam et al. 1992) plotted to illustrate the similarity of leaf blade growth rate over time in the two studies. **b** Activity of soluble plus ionically bound apoplastic peroxidase (*APOD*) from a previous study (MacAdam et al. 1992) and concentration of ferulate (*FA*), diferulates (*DFA*), and *p*-coumarate (*pCA*) from the current study for genetically identical low-LER leaf blades grown under similar conditions of daylength, light and temperature. Peroxidases were extracted from the cell wall space (apoplast) of intact 5-mm-long leaf blade segments by vacuum infiltration and low-speed centrifugation

ionically bound cell wall peroxidases at the onset of diferulate formation and lignin deposition in oat coleoptiles. Ikegawa et al. (1996) found that a transient increase of ionically bound cell wall peroxidase occurred 36 h after infection of resistant oat leaves with crown rust (*Puccinia coronata* f. sp. *avenae*) and coincided with an increase in diferulic acid in the hemicellulose fraction of oat cell walls.

*In conclusion*, our data support the hypotheses of Fry (1979) and Musel et al. (1997) that ferulate dimerization and the onset of lignification are associated with cessation of segmental elongation in grasses. Further work is, however, required to clearly demonstrate that ferulate cross-linking and lignification are agents responsible for cessation of leaf growth in grasses.

**Acknowledgements** This research was a joint contribution of the Utah Agricultural Experiment Station, approved as journal paper no. 7207, and USDA-ARS. Mention of a trademark or proprietary product does not constitute a guarantee or warranty of the product by the USDA and does not imply its approval to the exclusion of other products that may also be suitable.

## References

- Carmona MJ, Cuadrado A (1986) Analysis of growth components in *Allium* roots. *Planta* 168:183–189
- de Souza IRP, MacAdam JW (1998) A transient increase in apoplastic peroxidase activity precedes decrease in elongation rate of B73 maize (*Zea mays*) leaf blades. *Physiol Plant* 104:556–562
- de Souza IRP, MacAdam JW (2001) Gibberellic acid and dwarfism effects on the growth dynamics of B73 maize (*Zea mays* L.) leaf blades: a transient increase in apoplastic peroxidase activity precedes cessation of cell elongation. *J Exp Bot* 52:1–10
- Elder T, Ede, RM (1995) Coupling of coniferyl alcohol in the formation of dilignols: a molecular orbital study. In: Proceedings of the 8th international symposium of wood and pulping chemistry, vol 1. Gummerus Kirjapaino Oy, Helsinki, Finland, pp 115–122
- Erickson, RO (1976) Modeling of plant growth. *Annu Rev Plant Physiol* 27:407–434
- Fry SC (1979) Phenolic components of the primary cell wall and their possible role in the hormonal regulation of growth. *Planta* 146:343–351
- Fry SC, Willis SC, Paterson AEJ (2000) Intraprotoplasmic and wall-localised formation of arabinoxylan-bound diferulates and larger ferulate coupling-products in maize cell-suspension cultures. *Planta* 211:679–692
- Gonzalez LF, Rojas MC (1999) Role of wall peroxidases in oat growth inhibition by DIMBOA. *Phytochemistry* 50:931–937
- Gonzalez LF, Cecilia Rojas, M, Perez FJ (1999) Diferulate and lignin formation is related to biochemical differences of wall-bound peroxidases. *Phytochemistry* 50:711–717
- Grabber JH, Hatfield RD, Ralph J, Zon J, Amrhein N (1995) Ferulate cross-linking in cell walls isolated from maize cell suspensions. *Phytochemistry* 40:1077–1082
- Grabber JH, Quideau S, Ralph J (1996) *p*-Coumaroylated syringyl units in maize lignin; implications for  $\beta$ -ether cleavage by thioacidolysis. *Phytochemistry* 43:1189–1194
- Grabber J H, Hatfield RD, Ralph J (1998a) Diferulate cross-links impede the enzymatic degradation of nonlignified maize walls. *J Sci Food Agric* 77:193–200
- Grabber J H, Ralph J, Hatfield RD (1998b) Ferulate cross-links limit the enzymatic degradation of synthetically lignified primary walls of maize. *J Agric Food Chem* 46:2609–2614
- Grabber JH, Ralph J, Hatfield RD (2000) Cross-Linking of maize walls by ferulate dimerization and incorporation into lignin. *J Agric Food Chem* 48:6106–6113
- Hanley AB, Russell WR, Chesson A (1993) Formation of substituted truxillic and truxinic acids in plant cell walls – a rationale. *Phytochemistry* 33:957–960
- Hartley RD, Morrison III WH, Baliza F, Towers GHN (1990) Substituted truxillic and truxinic acids in cell walls of *Cynodon dactylon*. *Phytochemistry* 29:3699–3703
- Hatfield RD, Ralph J. (1999) Modeling the feasibility of intramolecular dehydrodiferulate formation in grass walls. *J Sci Food Agric* 79:425–427
- Ikegawa T, Mayama S, Nakayashiki H, Kato H (1996) Accumulation of diferulic acid during the hypersensitive response of oat leaves to *Puccinia coronata* f.sp. *avenae* and its role in the resistance of oat tissues to cell wall degrading enzymes. *Physiol Mol Plant Pathol* 48:245–255
- Ishii T (1991) Isolation and characterization of a diferuloyl arabinoxylan hexasaccharide from bamboo shoot cell-walls. *Carbohydr Res* 219:15–22
- Jacquet G, Pollet B, Lapierre C (1995) New ether-linked ferulic acid-coniferyl alcohol dimers identified in grass straws. *J Agric Food Chem* 43:2746–2751
- Jones RJ, Nelson CJ, Slesper DA (1979) Seedling selection for morphological characters associated with yield of tall fescue. *Crop Sci* 19:631–634
- Jung HG, Morrison TA, Buxton DR (1998) Degradability of cell-wall polysaccharides in maize internodes during stalk development. *Crop Sci* 38:1047–1051
- Kamisaka S, Takeda S, Takahashi K, Shibata K (1990) Diferulic and ferulic acid in the cell wall of *Avena* coleoptiles – their relationships to mechanical properties of the cell wall. *Physiol Plant* 78:1–7
- Kawamura Y, Wakabayashi K, Hoson T, Yamamoto R, Kamisaka S (2000) Stress-relaxation analysis of submerged and air-grown rice coleoptiles: correlations with cell wall biosynthesis and growth. *J Plant Physiol* 156:689–694
- Lu F, Ralph J (1999) Detection and determination of *p*-coumaroylated units in lignins. *J Agric Food Chem* 47:1988–1992
- MacAdam JW, Nelson CJ (1987) Specific leaf weight in zones of cell division, elongation and maturation in tall fescue leaf blades. *Ann Bot* 59:369–376
- MacAdam JW, Volenec JJ, Nelson CJ (1989) Effects of nitrogen on mesophyll cell division and epidermal cell elongation in tall fescue leaf blades. *Plant Physiol* 89:549–556
- MacAdam JW, Sharp RE, Nelson CJ (1992) Peroxidase activity in the leaf elongation zone of tall fescue. II. Spatial distribution of apoplastic peroxidase activity in genotypes differing in length of the elongation zone. *Plant Physiol* 99:879–885
- Markwalder HU, Neukom H (1976) Diferulic acid as a possible crosslink in hemicelluloses from wheat germ. *Phytochemistry* 15:836–837
- Migne C, Prentier G, Utille JP, Angibeaud P, Cornu A, Grenet E (1998) Immunocytochemical localisation of *para*-coumaric acid and feruloyl-arabinose in the cell walls of maize stem. *J Sci Food Agric* 78:373–381
- Morrison TA, Jung HG, Buxton DR, Hatfield RD (1998) Cell-wall composition of maize internodes of varying maturity. *Crop Sci* 38:455–460
- Musel G, Schindler T, Bergfeld R, Ruel, K, Jacquet G, Lapierre C, Speth V, Schopfer P (1997) Structure and distribution of lignin in primary and secondary cell walls of maize coleoptiles analyzed by chemical and immunological probes. *Planta* 201:146–159
- Myton KE, Fry SC (1995) Dithiothreitol and cobalt effects on membrane-associated peroxidases oxidizing feruloyl-CoA. *Phytochemistry* 38:573–577
- Ralph J, Hatfield RD, Quideau S, Helm RF, Grabber JH, Jung HJG (1994a) Pathway of *p*-coumaric acid incorporation into maize lignin as revealed by NMR. *J Am Chem Soc* 116:9448–9456
- Ralph J, Quideau S, Grabber JH, Hatfield RD (1994b) Identification and synthesis of new ferulic acid dehydrodimers present in grass cell walls. *J Chem Soc Perkins Trans* 1 3485–3498
- Russell W R, Forrester AR, Chesson A, Burkitt M J (1996) Oxidative coupling during lignin polymerization is determined by unpaired electron delocalization within parent phenylpropanoid radicals. *Arch Biochem Biophys* 332:357–366
- Schaefer VJ, Harker D (1942) Surface replicas for use in the electron microscope. *J Appl Phys* 13:427–433
- Schnyder H, Seo S, Rademacher IF, Kühbauch W (1990) Spatial distribution of growth rates and of epidermal cell lengths in the elongation zone during leaf development in *Lolium perenne* L. *Planta* 181:423–431
- Schopfer P (1996) Hydrogen peroxide-mediated cell-wall stiffening in vitro in maize coleoptiles. *Planta* 199:43–49
- Schopfer P, Lapierre C, Nolte, T (2001) Light-controlled growth of the maize seedling mesocotyl: mechanical cell-wall changes in the elongation zone and related changes in lignification. *Physiol Plant* 111:83–92
- Scobbie L, Russell W, Provan GJ, Chesson A (1993) The newly extended maize internode: a model for the study of secondary cell wall formation and consequences for digestibility. *J Sci Food Agric* 61:217–225
- Scott BIH, Gulline H, Pallaghy CK (1968) The electrochemical state of cells of broad bean roots I. Investigations of elongating roots of young seedlings. *Aust J Biol Sci* 21:185–200
- Silk WK, Lord EM, Eckard KJ (1989) Growth patterns inferred from anatomical records. Empirical tests using longisections of roots of *Zea mays* L. *Plant Physiol* 90:708–713



- Tan K-S, Hoson T, Masuda Y, Kamisaka S (1991) Correlation between cell wall extensibility and the content of diferulic and ferulic acids in cell walls of *Oryza sativa* coleoptiles grown under water and in air. *Physiol Plant*. 83:397–403
- Tan K-S, Hoson T, Masuda Y, Kamisaka S (1992) Involvement of cell wall-bound diferulic acid in light-induced decrease in growth rate and cell wall extensibility of *Oryza* coleoptiles. *Plant Cell Physiol* 33:103–108
- Terashima N, Fukushima K, He LF, Takabe K (1993) Comprehensive model of the lignified plant cell wall. In: Jung HG, Buxton DR, Hatfield RD, Ralph J (eds) *Forage cell wall structure and digestibility*. ASA-CSSA-SSSA, Madison, pp 247–270
- Vailhé MAB, Provan GJ, Scobbie L, Chesson A, Maillot MP, Cornu A, Besle JM (2000) Effect of phenolic structures on the degradability of cell walls isolated from newly extended apical internode of tall fescue (*Festuca arundinacea* Schreb.). *J Agric Food Chem* 48:618–623
- Vassey, TL (1986) Morphological, anatomical, and cytohistological evaluations of terminal and axillary meristems of tall fescue. PhD thesis, University of Missouri, Columbia, USA
- Wakabayashi K, Hoson T, Kamisaka S (1997) Osmotic stress suppresses cell wall stiffening and the increase in cell wall-bound ferulic and diferulic acids in wheat coleoptiles. *Plant Physiol* 113:967–973